Post-translational Regulation of the *Arabidopsis* Circadian Clock through Selective Proteolysis and Phosphorylation of Pseudo-response Regulator Proteins

Sumire Fujiwara, Lei Wang, Linqu Han,
Sung-Suk Suh, Patrice A. Salomé, C.
Robertson McClung and David E. Somers

Access the most updated version of this article at doi: 10.1074/jbc.M803471200

Find articles, minireviews, Reflections and Classics on similar topics on the JBC Affinity Sites.

Alerts:

- When this article is cited
- When a correction for this article is posted

Click here to choose from all of JBC's e-mail alerts

Supplemental material:

http://www.jbc.org/content/suppl/2008/06/19/M803471200.DC1.html

This article cites 59 references, 36 of which can be accessed free at
http://www.jbc.org/content/283/34/23073.full.html#ref-list-1

Post-translational Regulation of the *Arabidopsis* Circadian Clock through Selective Proteolysis and Phosphorylation of Pseudo-response Regulator Proteins*[S]

Sumire Fujiwara[‡1,2], **Lei Wang**[‡1], **Linqu Han**[‡3], **Sung-Suk Suh**[‡], **Patrice A. Salomé**[§4], **C. Robertson McClung**[§], **and David E. Somers**[‡5]

From the ‡Department of Plant Cellular and Molecular Biology/Plant Biotechnology Center, Ohio State University, Columbus, Ohio 43210 and the §Department of Biological Sciences, Dartmouth College, Hanover, New Hampshire 03755-3576

The circadian clock controls the period, phasing, and amplitude of processes that oscillate with a near 24-h rhythm. One core group of clock components in *Arabidopsis* that controls the pace of the central oscillator is comprised of five PRR (pseudo-response regulator) proteins whose biochemical function in the clock remains unclear. Peak expression of TOC1 (timing of cab expression 1)/PRR1, PRR3, PRR5, PRR7, and PRR9 are each phased differently over the course of the day and loss of any PRR protein alters period. Here we show that, together with TOC1, PRR5 is the only other likely proteolytic substrate of the E3 ubiquitin ligase SCF^{ZTL} within this PRR family. We further demonstrate a functional significance for the phosphorylated forms of PRR5, TOC1, and PRR3. Each PRR protein examined is nuclear-localized and is differentially phosphorylated over the circadian cycle. The more highly phosphorylated forms of PRR5 and TOC1 interact best with the F-box protein ZTL (ZEITLUPE), suggesting a mechanism to modulate their proteolysis. *In vivo* degradation of both PRR5 and ZTL is inhibited by blue light, likely the result of blue light photoperception by ZTL. TOC1 and PRR3 interact *in vivo* and phosphorylation of both is necessary for their optimal binding *in vitro*. Additionally, because PRR3 and ZTL both interact with TOC1 *in vivo* via the TOC1 N terminus, taken together these data suggest that the TOC1/PRR3 phosphorylation-dependent interaction may protect TOC1 from ZTL-mediated degradation, resulting in an enhanced amplitude of TOC1 cycling.

The rotation of the earth on its axis yields dramatic diurnal changes in the environment. This periodic environmental change has driven the evolution of an internal timekeeping mechanism, the circadian clock, to allow the prediction of impending environmental change and synchronization with this 24-h environmental periodicity. The possession of an internal circadian clock that resonates with the environmental period enhances fitness and impaired clock function confers a striking loss of fitness (1). In plants this includes greatly reduced net photosynthesis and increased mortality (2, 3).

At the core of the eukaryotic clock are one or more autoregulatory negative feedback loops: clock genes are transcribed and transcripts are translated into proteins that inhibit further transcription. Degradation of both mRNA and protein relieves this inhibition and the cycle renews. One of the feedback loops of the *Arabidopsis thaliana* clock has two partially redundant single Myb domain transcription factors, circadian clock associated 1 (CCA1)[6] and late elongated hypocotyl (LHY), negatively regulating the transcription of *TOC1* (4). Current models of the *Arabidopsis* clock propose two to three additional negative feedback loops interlocked with the initial CCA1/LHY/TOC1 loop (5, 6).

TOC1 encodes a pseudo-response regulator (PRR), and is the founding member of a family of *PRR* genes that contribute to the *Arabidopsis* circadian clock. Transcript abundance of each of five *PRR* genes oscillates in circadian fashion, peaking sequentially from shortly after dawn to approximately dusk in the order *PRR9-PRR7-PRR5-PRR3-TOC1/PRR1* (7). Loss of function for each of the *PRR* genes alters circadian period phenotypes, with *toc1*, *prr3*, and *prr5* mutations shortening periods and *prr7* and *prr9* mutations lengthening periods (8–16). CCA1 and LHY serve as positive regulators of *PRR7* and *PRR9*, which in turn negatively regulate *CCA1* and *LHY* (12, 14, 17). *PRR7* and *PRR9* are partially redundant with each other and with *PRR5*, because the double *prr7 prr9* mutant shows extreme period lengthening, more than can be accounted for by additive interaction of the two single mutants (11, 12, 14), and the triple *prr5 prr7 prr9* mutant is arrhythmic and exhibits constitutive *CCA1* expression.

Recently post-transcriptional and post-translational processes, such as phosphorylation and clock-regulated proteolysis

of oscillator proteins, have been found to be critical for proper clock function in a number of eukaryotes (18–24). In *Arabidopsis*, CCA1 phosphorylation by casein kinase 2 is essential for its role in the clock (25–27). Similarly, proteasome-dependent proteolysis post-translationally controls the levels of ancillary or core clock components in *Arabidopsis*, such as LHY, a subunit of casein kinase 2 (CKB4), GIGANTEA (GI), and ZTL (28–31). Additionally, the E3 ubiquitin ligase SCF^{ZTL} targets TOC1 and PRR5 proteins for degradation (32–35). As the five PRR proteins share two highly conserved domains, the pseudo-receiver (PR) and the CONSTANS, CONSTANS-LIKE, and TOC1 (CCT) domains, we investigated whether ZTL may target a greater set of these proteins for proteasome-dependent degradation, and how their phosphorylation state affects their stability.

Here we establish that the five *PRR* family proteins cycle with a slightly lagging phase relative to respective transcripts. All of the PRR proteins examined are nuclear-localized and phosphorylated, and many of them become progressively phosphorylated over the circadian cycle, with maximum phosphorylation prior to degradation. We show that TOC1/PRR1 and PRR5 are likely the only PRR proteins of this family proteolytically controlled directly by SCF^{ZTL}, but that ZTL indirectly controls PRR9 protein levels. A second post-translational process, phosphorylation, controls TOC1 and PRR3 interaction *in vivo* via the TOC1 N terminus. Our data suggests a complex post-translational relationship between TOC1, PRR3, and ZTL that helps establish a strong amplitude to TOC1 cycling.

EXPERIMENTAL PROCEDURES

Plant Materials and Growth Conditions—Construction of the *TOC1-YFP* minigene (TMG) in the *Arabidopsis* wild type (WT) (TMG WT) and *ztl* mutant (TMG *ztl-3*) backgrounds have been described previously (33). The genomic fragments for *PRR3*, *PRR5*, *PRR7*, and *PRR9* (generically *PRRn*), containing the full promoter, 5′-untranslated region, and coding sequences up to the last codon before the STOP codon, were amplified by PCR with ExTaq (Takara Bio USA, Madison, WI) and subcloned into pGEM-T Easy (Promega, Madison, WI). The *PRR:PRRn* genomic fragments were then subcloned into the Gateway Entry vector pENTR-1A, and placed upstream of the green fluorescent protein (GFP) by LR recombination (Invitrogen) into the binary vector pMDC206 (36) according to the manufacturer's instructions. The genomic sequences cloned upstream of GFP were: −1431 to +2285 bp (*PRR3*), −5116 to +2340 bp (*PRR5*), −1194 to +3176 bp (*PRR7*), and −1541 to +2025 bp (*PRR9*). Plants were transformed by floral dip (37) via *Agrobacterium tumefaciens* strain GV3101. Primary transformants were selected for hygromycin resistance, and allowed to self-pollinate. *PRR:PRRn-GFP* constructs were transformed into WT *Arabidopsis* (Col) and *ztl-1* (Col), backgrounds as described in the text, and multiple transformants were identified and characterized for each construct. One to three similarly expressing lines were chosen for the experiments presented.

TOC1 full-length, N-terminal (1–243) and C-terminal (243–648) constructs were obtained using the primers: TOC1-1-F: 5′-GTG GTA CCA TGG ATT TGA ACG GTG-3′; TOC1–740-F: 5′-ACG GTA CCA TGA AAA GAA ATA GTA AT-3′; TOC1–760-R: 5′-ACT CGA GAT TAC TAT TCT TTT CA-3′; TOC1–1864-R: 5′-TCT CGA GAG TTC CCA AAG CAT CAT CC-3′. TOC1-1-F and TOC1–1864-R, TOC1-1-F and TOC1–760-R, and TOC1–740-F and TOC1-1864-R combinations were used to obtain full-length TOC1, TOC1 N- and C-terminal fragments, respectively. Each was subcloned into pENTR-2B and pENTR-3C, and placed upstream (N-TAP) or downstream (C-TAP) of the TAP tag by LR recombination (Invitrogen) into the binary vector pCD3–696 (N-TAP) or pCD3–679 (C-TAP) according to the manufacturer's instructions.

prr5-1 (SALK_006280; (16)) was crossed to *toc1-21* (Ws-2; (38)), to *prr3-1* (SALK_090261; (10)), and to *ztl-3* (SALK_035701; (31)) and PCR-based scoring was used to identify *prr5-1 toc1-21*, *prr5-1 prr3-1*, and *prr5-1 ztl-3*, respectively. Progeny from a WT Col/Ws-2 F2 segregant were used as a control for potential endogenous period differences between the two WT parents.

Arabidopsis seedlings were grown under 12-h white fluorescent light (50–60 μmol m^{-2} s^{-1})/12 h dark cycles for 8–12 days on MS (Murashige and Skoog) plates with 3% sucrose and 1% agar as previously described (39). Red (30 μmol m^{-2} s^{-1}) and blue (25 μmol m^{-2} s^{-1}) light treatments were conducted in a Percival E30LEDL3 growth chamber (Percival Scientific, Perry, IA). Period estimates from luciferase-based imaging were based on *CAB2:luciferase* reporters.

Immunolocalization—Immunodetection of GFP in seedlings was performed following adapted protocols (40, 41). Eight-day old seedlings grown under LD cycles were fixed for 3 h in 4% paraformaldehyde in 1× PBS at 4 °C. Following three 15-min washes in 1× PBS, 0.1% Triton X-100 and three 15-min washes in water, cell wall was digested in 1% cellulase, 1% macerozyme in 1× PBS for 45 min with shaking. After three washes in 1× PBS, 0.01% Triton X-100, seedlings were incubated in blocking buffer (5% bovine serum albumin in 1× PBS) for 2 h at room temperature, followed by incubation with the primary antibody (ab290, Abcam, Cambridge, MA) diluted at 1:250 in 2% bovine serum albumin, 1× PBS with gentle shaking overnight at 4 °C. The next day, seedlings were washed four times, 15 min each, in 1× PBS, 0.01% Triton X-100, before incubation with secondary antibody (goat anti-rabbit, Alexa Fluor-488 conjugated, Molecular Probes, Eugene, OR), diluted to 1:400 in 2% bovine serum albumin, 1× PBS. After four 15-min washes in 1× PBS, 0.01% Triton X-100, seedlings were mounted in Mount Quick (Electron Microscopy Sciences, Washington, PA).

Cycloheximide Treatments—Plants grown under LD cycles for 10 days were transferred to continuous white, red, blue light, or dark at ZT0 and transferred into liquid MS media with 0.01% Triton X-100 and 100 μM cycloheximide at CT7 or CT19. Plants were immersed in the media and shaken slowly for the indicated durations before harvesting.

Protein Extraction and Immunoblot Analysis—Protein extraction for TOC1-YFP, PRR3-GFP, PRR5-GFP, PRR7-GFP, and PRR9-GFP detection was performed as described previously (42). Protein extraction for ZTL detection was described previously (31). Immunoprecipitations of PRR5-GFP, PRR3-GFP, or TMG and co-immunoprecipitation of ZTL were performed as described previously with minor modifications (42).

0.5 μl of anti-GFP polyclonal antibody (ab290, Abcam) was incubated with 12 μl of protein A-agarose (Invitrogen) made to a final volume of 25 μl at 4 °C for 2 h. Proteins were extracted from 500 μl of ground tissue using 500 μl of immunoprecipitation buffer, and the extract was added to the affinity matrix and incubated for 1.5 h with gentle rotation. Immunoblot analysis was performed as described previously (42).

GST Binding Assay—GST and GST-ZTL were expressed in *Escherichia coli* BL21(DE3) and purified with glutathione-agarose (Sigma). Concentration of each protein bound to the glutathione-agarose was determined by Coomassie staining. Equal amounts of glutathione beads of GST and GST-ZTL were used for the *in vitro* binding assay. Seedlings were entrained in LD cycles and harvested at ZT13 on day 10. Frozen samples were ground in liquid nitrogen, the protein was extracted with ice-cold buffer A (50 mM Tris-Cl, pH 7.5, 150 mM NaCl, 0.5% Nonidet P-40, 1 mM EDTA, 3 mM dithiothreitol, 1 mM phenylmethylsulfonyl fluoride, 5 μg/ml leupeptin, 1 μg/ml aprotinin, 1 μg/ml pepstatin, 5 μg/ml antipain, 5 μg/ml chymostatin, 50 μM MG132, 50 μM MG115, 50 μM ALLN), and incubated 90 min at 4 °C with GST and GST-ZTL glutathione-agarose, respectively. The beads were washed with buffer I (50 mM Tris-Cl, pH 7.5, 150 mM NaCl, 1 mM EDTA, 3 mM dithiothreitol, 1 mM phenylmethylsulfonyl fluoride, 0.5% Nonidet P-40, and 0.5% Triton X-100) for 20 min, followed by buffer II (buffer I with 0.1% Nonidet P-40 and 0.1% Triton X-100) for 10 min, and buffer III (buffer I without detergents) for 5 min. Bound protein was eluted in SDS sample buffer and size-fractionated on 8% SDS-PAGE (acrylamide:bisacrylamide, 149:1) and analyzed by immunoblot.

Phosphatase Assays—For binding assays, protein was extracted with ice-cold buffer A with 2.5 mM MnCl$_2$ added. 4,000 units of λ-protein phosphatase (New England Biolabs) were added to 1 ml of soluble extracts. The mixture was incubated at 30 °C for 15 min. Samples were loaded into 8% SDS-PAGE (acrylamide:bisacrylamide, 149:1) and analyzed by immunoblot. For PRR phosphorylation tests, protein extracts were prepared in 1× λ-phosphatase buffer supplemented with 2.5 mM MnCl$_2$, 0.5% Triton X-100, 0.4% Nonidet P-40, 2.5 μg/ml antipain, 2.5 μg/ml chymostatin, 1 μg/ml pepstatin, 5 μg/ml leupeptin, 5 μg/ml aprotinin, 25 mM phenylmethylsulfonyl fluoride and proteasome inhibitors as described above. Forty to fifty-microliter aliquots of the resulting protein extracts were incubated with 400 units of λ-protein phosphatase at 30 °C for 15 min. Calf intestine alkaline phosphatase (CIP) assays were performed using protein extract prepared in New England Biolabs buffer 3 supplemented with protease inhibitors and proteasome inhibitors as described above. Forty-microliter aliquots of the resulting protein extracts were incubated with 10 units of CIP (New England Biolabs) with or without phosphatase inhibitors (NaF/Na$_3$VO$_4$) at 37 °C for 15 min.

Transient Expressions and Immunoprecipitations—Assays using co-infiltrated *Agrobacterium*-mediated protein expression in *Nicotiana benthamiana* have been described previously (42). All constructs were 35S cauliflower mosaic virus promoter-driven, except ZTL, which was a native promoter-driven genomic clone (39). For TAP-TOC1/PRR3 assays, total *N. benthamiana* protein was extracted post-infiltration with ice-

cold buffer A using 300 μl of tissue, and 600 μl of cleared supernatant was incubated with 25 μl of human IgG-agarose at 4 °C for 90 min. After rinses, the resin was further treated with or without protein phosphatase prior to subsequent immunoprecipitations. The resin was rinsed with protein phosphatase buffer, and incubated with λ-protein phosphatase (400 units) at 30 °C for 15 min. For immunoprecipitations, total protein was extracted from PRR3-GFP *Arabidopsis* at the required time points. For dephosphorylation tests of PRR3-GFP, CIP was used as described above. Extracts were incubated with the previously prepared TAP-TOC1-loaded resin. After incubation at 4 °C (90 min), the resin was rinsed and Precision protease (0.5 μl) was added to release TOC1-TAP and associated proteins, and the supernatant was separated by SDS-PAGE. Immunoblot detection was as previously described.

Reverse Transcriptase-PCR—Reverse transcriptase-PCR was performed using cDNA from WT and *ztl* tissue to detect endogenous *PRR* gene expression using the following primers and conditions: *TOC1*, 52 °C, 5′-GTT AGG AAG ATG AAC GGC GTG A-3′ and 5′-AAG TTG AGC CGC AAG AGC CA-3′; *PRR3*, 53 °C, 5′-GTC GGT GAT CGA AGT GTG TTG AG-3′ and 5′-GGA GGT TCT CTC TTC TAT ACC AA-3′; *PRR5*, 53 °C, 5′-GTT CCA TGG ATG TAG ATG AGA GG-3′ and 5′-GTA CAA AGA ACA GCT CCT GCA TC-3′; *PRR7*, 53 °C, 5′-CCG CTG CAA CTG ATG ATA AC-3′ and 5′-AAC CAG ACC AGA CAA CGA CA-3′; *PRR9*, 53 °C, 5′-GCC AGA GAG AAG CTG CAT TG-3′ and 5′-CTG AGA AGA AGA AGC CAA TCA A-3′. *ACTIN* was used as a control and amplified simultaneously within each reaction as described previously (42).

Accession Numbers—*Arabidopsis* Genome Initiative locus identifiers for the genes mentioned in this study are as follows: *CCA1* (At2g46830), *FKF1* (At1g68050), *GI* (At1g22770), *LHY* (At1g01060), *LKP2* (At2g18915), *PRR3* (At5g60100), *PRR5* (At5g24470), *PRR7* (At5g02810), *PRR9* (At2g46790), *TIR1* (At3g62980), *TOC1/PRR1* (At5g61380), and *ZTL* (At5g57360).

RESULTS

Cyclic Expression of the PRR Proteins Lags behind the Respective Message Rhythms—TOC1 is the founding member of a five-member family of PRR and is a proteolytic target of the clock-related F-box protein ZTL. To determine whether other PRR/TOC1 family members are additional targets, we first characterized their endogenous protein expression pattern. C-terminal GFP fusions were made to the genomic sequences of PRR3, 5, 7, and 9 and stably transformed into *Arabidopsis* under the expression of each respective native promoter (*PRR*::*PRRn-GFP*). Multiple independent transformants were obtained for each construct and representative expression patterns for each are shown in Fig. 1. The period of each transgenic line chosen is slightly different from WT and generally in the opposite direction of the period effects of the known loss-of-function mutants of each gene (supplemental Table S1), consistent with the expected effects of slightly elevated expression. Free-running periods of *PRR3*::*PRR3-GFP* transformants are 1–1.5 h longer than WT in red and blue light, consistent with the slightly shorter period of the *prr3* mutant (10). *PRR5*::*PRR5-GFP* transformants are 2–2.5 h longer than
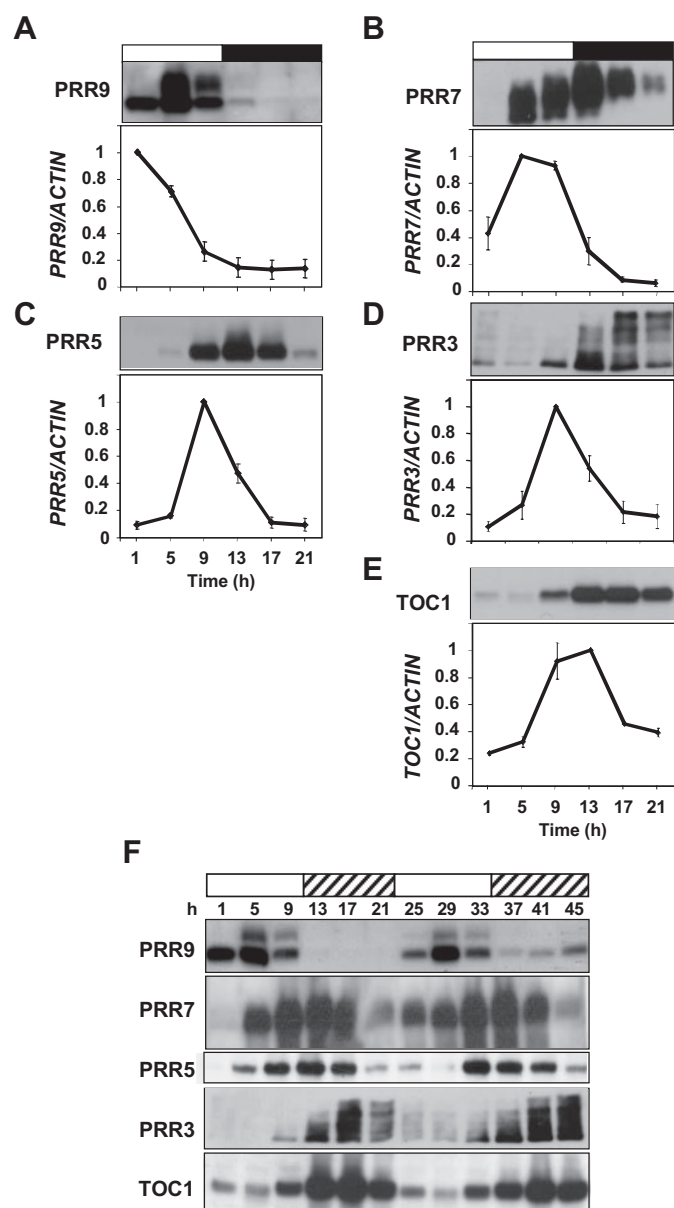
FIGURE 1. **Diurnal and circadian cycling of PRR levels.** Extracts from seedlings entrained under LD cycles (*A–E*) or entrained and released into constant white light (*F*) were processed for soluble protein (*A–F*) and total RNA (*A–E*), subjected to immunoblotting and probed with anti-GFP antibody (*upper part of each panel*) or subjected to low cycle semi-quantitative reverse transcriptase-PCR (*lower part of each panel*). *A–E*, PRR-GFP protein levels and quantitation of endogenous *PRR* message abundance for each *PRR* gene is indicated. *F*, free-running rhythm of PRR-GFP protein expression in constant light. Equal protein loading (60 μg) in all immunoblot lanes. *PRR* mRNA expressed relative to *ACTIN. Light* and *dark bars above* each panel indicates light and dark growth periods, respectively. *Hatched boxes* indicate subjective night. *h* is time in hours. Each experiment was repeated at least three times with similar results. Means of three trials ± S.E. are shown.

WT, consistent with the more severe shortening effect seen in *prr5* mutants (8, 10, 16). The *PRR7::PRR7-GFP* transformants are slightly longer than WT in red and blue light, similar to long period of *prr7* mutants. This unexpected finding has also been reported in plants strongly (43) and weakly (44) overexpressing PRR7, suggesting a complex relationship between PRR7 levels and period. *PRR9::PRR9-GFP* plants are similar to WT in red light, and slightly shorter in blue light,

consistent with the long period of *prr9* mutants in white light. Together these results indicate that each fusion protein is functional.

The abundance of each of the PRR proteins oscillates under diurnal cycles with a peak expression often lagging 4–8 h after the expression peaks of the respective message levels (Fig. 1). Notably, PRR9 and PRR3 persist at high levels well past the peak of mRNA expression and diminish rapidly upon transition to dark or light, respectively (Fig. 1, *A* and *D*) (45). To determine whether these declines are due to light/dark transitions, we tested expression under constant white light (LL) (Fig. 1*E*). In LL all five proteins continue to cycle very robustly, consistent with previous reports of circadian expression of *PRR* message levels (7). These results imply a rapid turnover of the five PRR proteins and confirm and extend previous reports (44, 45).

Nuclear Localization of PRR Proteins—TOC1 (PRR1) has been shown in transient assays to be nuclear-localized (46). We tested whether other PRR proteins were similarly present in the nucleus. Representative lines expressing PRR3-GFP, PRR5-GFP, and PRR7-GFP under the respective endogenous promoters and grown under light/dark cycles were harvested and fixed at times of strong abundance (between ZT 8 and 12) and immunolocalized through the GFP moiety (Fig. 2). All three proteins are distinctly and strongly nuclear-localized in the shoot meristem (Fig. 2, *D–M*). In all other tissues tested (leaf mesophyll and vasculature, and root meristems) nuclear localization was also distinct (Fig. 2, *N–R*). These findings are consistent with transient localization assays using strong ectopic promoters (35S cauliflower mosaic virus) (47), and suggest a nuclear function for all four of the PRR proteins tested here.

TOC1 and PRR5 Are the Sole Proteolytic Targets of ZTL within the PRR Family—To determine whether ZTL might target members of the PRR family beside TOC1, independent transformations of the each of the *PRR::PRR-GFP* constructs were made into the *ztl-1* background. The single missense mutation in the kelch domain in *ztl-1* is functionally equivalent to a *ztl* null mutation, but has WT levels of the ZTL protein (39, 48). One line showing a representative expression pattern was chosen for each *PRR* construct for further analysis.

All *PRR9::PRR9-GFP* lines showed little to no expression of PRR9-GFP protein (data not shown). We examined mRNA expression patterns of the transgene and of endogenous *PRR9* in *ztl-1* and found very low expression of both in all lines tested (Fig. 3*A*). Because enhanced accumulation of TOC1 occurs in the absence of ZTL (33), this result is consistent with a previous report showing that strong expression of TOC1 severely depresses *PRR9* message levels (49). Due to this strong negative regulation of *PRR9* expression in *ztl* mutants we were unable to examine the direct effect of reduced ZTL on PRR9 protein. This result, together with the anti-phase expression of *PRR9* mRNA and ZTL protein strongly suggests that PRR9 is not a substrate of ZTL.

Of the remaining four PRRs, PRR3 and PRR7 protein showed similar amplitude and patterns of rhythmic expression in the *ztl-1* and WT backgrounds (compare Fig. 1, *B* and *D*, with Fig. 3*B*). We tested whether PRR3 or PRR7 interact with ZTL *in vivo* through co-immunoprecipitation tests. Using *PRR3::PRR3-GFP* expressing plants, under no circumstances
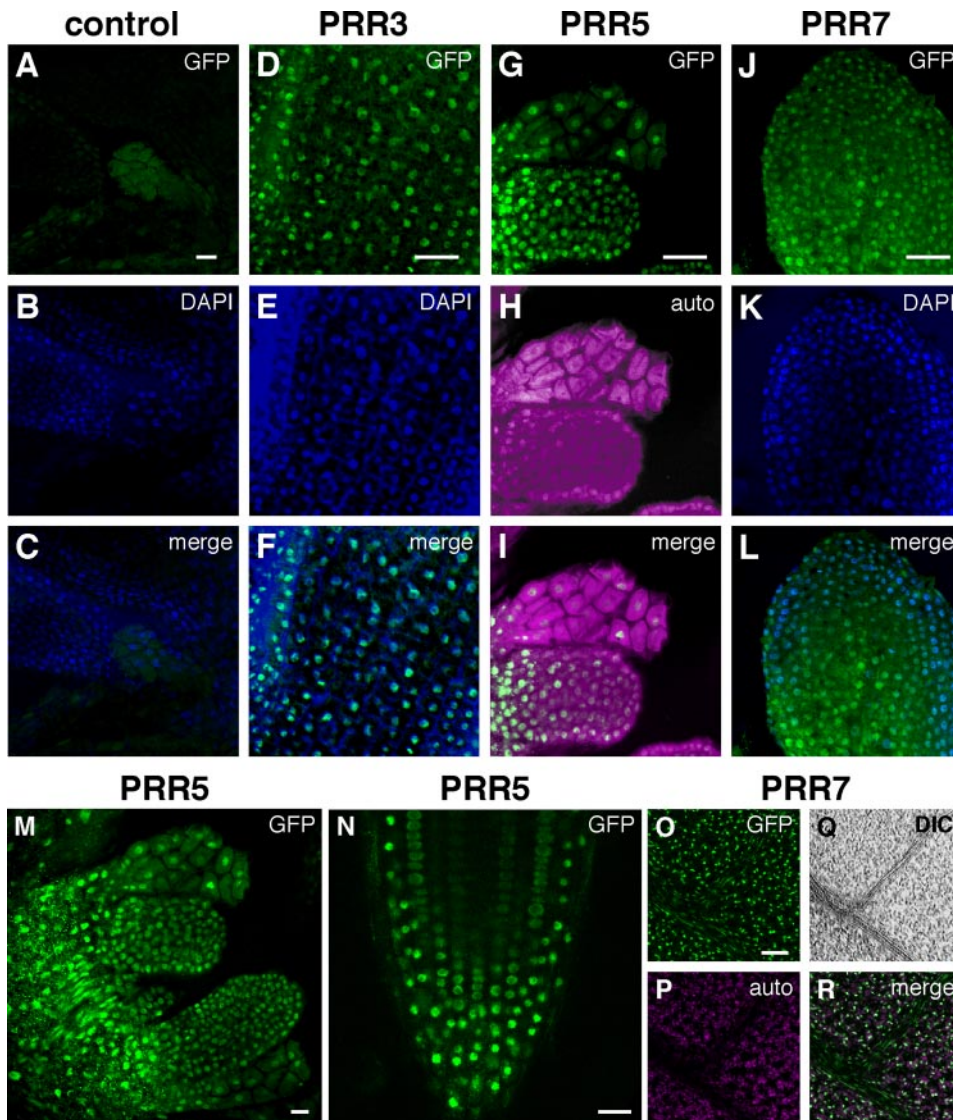
FIGURE 2. **PRR3, PRR5, and PRR7 are nuclear proteins.** Seedlings carrying C-terminal GFP fusions of the indicated PRR, placed under the control of their endogenous promoter, were entrained to LD cycles, and fixed in 4% paraformaldehyde at ZT8–12. GFP was detected with a rabbit polyclonal GFP antibody, followed by a goat anti-rabbit antibody conjugated with Alexa Fluor 488. GFP was visualized using a Leica TCS SP microscope. All *scale bars* represent 10 μm. *A–C*, Columbia (*Col*) plants do not stain for the GFP antibody. Confocal images were taken sequentially for GFP (*A*) or 4′,6-diamidino-2-phenylindole (*DAPI*) (*B*) at the apex of a Col-2 seedling. The overlay of GFP and DAPI channels is shown in *C*. *D–F, PRR3::PRR3-GFP* localizes to the nucleus. *D*, GFP channel; *E*, DAPI channel; *F*, overlay. *G–I, PRR5::PRR5-GFP* localizes to the nucleus. *G*, GFP channel; *H*, autofluorescence signal; *I*, overlay. *J–L, PRR7::PRR7-GFP* localizes to the nucleus. *J*, GFP channel; *K*, DAPI channel; *L*, overlay. *M* and *N*, examples of *PRR5::PRR5-GFP* localization at the shoot (*M*) or root (*N*) apex. *O–R, PRR7::PRR7:GFP* localization in leaves. GFP signal (*O*) is detected in nuclei of both mesophyll and vasculature. *P*, chlorophyll autofluorescence; *Q*, differential interference contrast (*DIC*) image, showing the vasculature in the leaf; *R*, overlay of the GFP and chlorophyll channels.

protein (Fig. 3*B*) (33). Additionally, PRR5 shows strongly reduced rhythmic amplitude in *ztl-1*, with protein levels damping to high or intermediate levels, relative to WT (Fig. 3*B*). These results suggested that PRR5 may be an additional proteolytic target of ZTL, and we performed similar co-immunoprecipitation experiments using *PRR5::PRR5-GFP* expressing plants. Fig. 3*C* shows ZTL present in the immunoprecipitates at ZT9 and ZT17, indicating an interaction between the two at native expression levels, and that this interaction is stronger in the dark. The *ztl-1* mutation abrogates this interaction (Fig. 3*C*), similar to its effect on TOC1 (33). Taken together, these data strongly support full-length PRR5 as an endogenous interactor with ZTL, confirming and extending similar results using strong ectopic expressors or truncated versions of PRR5 (35).

We next tested whether PRR5 is also a substrate of the SCF^{ZTL} ubiquitin ligase. Cycloheximide (CHX) treatment of WT and *ztl-1* seedlings at two time points in constant light (subjective day, LL 7 and subjective night, LL 19) was used to determine whether PRR5-GFP undergoes differential degradation rates over the circadian cycle. PRR5-GFP is more rapidly degraded during the subjective night than during subjective day, with a half-life at LL19 of about 2.5 h compared with almost 9 h at LL7 (Fig. 3*D*). The greater stability early in the day is consistent with the very low levels of ZTL during this time (31). In the *ztl* mutant PRR5-GFP is significantly more stable during the subjective day and night, relative to the WT (Fig. 3*E*).

could we detect ZTL in co-immunoprecipitates with PRR3-GFP, or even in plants expressing PRR3 at very high levels (35S cauliflower mosaic virus::*GFP-PRR3*) (supplemental Fig. S1). We found similar results using *PRR7::PRR7-GFP* plants (data not shown). Additionally, the free-running period of the *prr5 prr3* double mutant is not additive but is indistinguishable from the short period *prr5* mutant, suggesting PRR3 acts upstream of PRR5, or it may act in support of PRR5 activity, but not independently of it (supplemental Fig. S2*C*).

In contrast, we confirm that TOC1 cycling is largely eliminated in the *ztl-1* mutant, due to the stabilization of the TOC1

These results, together with the physical interaction with ZTL, demonstrate that PRR5 is a proteolytic target of ZTL in light-grown plants, consistent with similar results reported for dark-grown etiolated seedlings or strong ectopic expressors of PRR5 (35). These findings are further supported by genetics, where the period of the double mutant *ztl-3 prr5* is intermediate between that of the *ztl* and *prr5* single mutants, consistent with PRR5 being one of at least two ZTL substrates (supplemental Fig. S2*A*). Similarly, if PRR5 and TOC1 are co-targets of the same SCF^{ZTL} complex then the *prr5 toc1* double mutant should be additively more severe than either single mutant alone. Con-
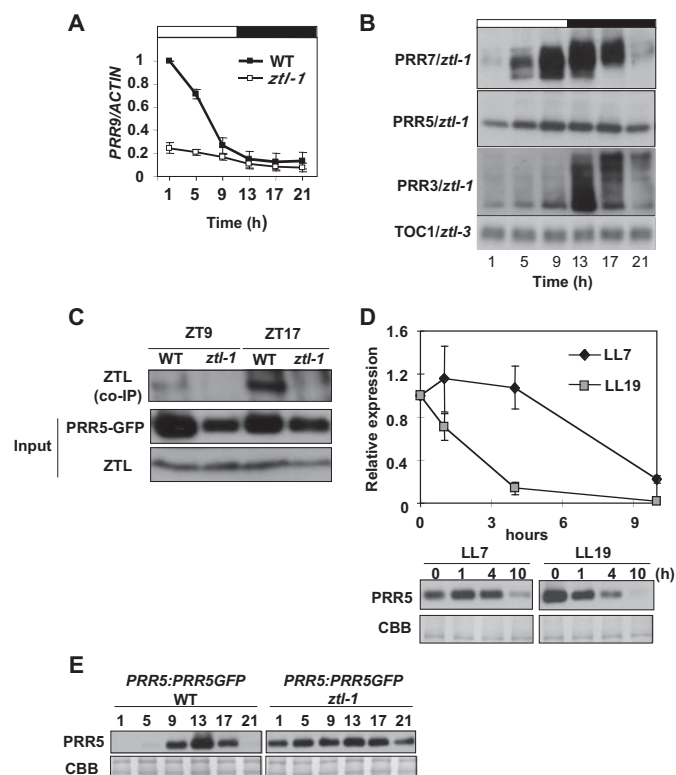
FIGURE 3. **TOC1 and PRR5 are the sole PRR direct targets of ZTL.** *A,* endogenous *PRR9* mRNA levels in WT and *ztl-1* plants. Extracts from seedlings entrained under LD cycles were processed for soluble protein and total RNA as described in the legend to Fig. 1. *B,* PRR-GFP expression profiles in the *ztl* mutant background. Ten-day-old plants grown under LD cycles were harvested at the times indicated. Equal protein was loaded (60 μg) in all immunoblot lanes. *C, in vivo* PRR5/ZTL interactions are abolished by the *ztl-1* mutation. Protein extracts were immunoprecipitated (*IP*) by anti-GFP antibodies and probed for co-immunoprecipitated ZTL. PRR5-GFP and ZTL levels present in the input are shown. Both were still present in post-binding supernatants (data not shown). *D,* PRR5 protein stability is under circadian regulation. Ten-day-old plants grown under LD cycles were transferred to continuous light at ZT0 and treated with 100 μM CHX at LL7 or LL19. Plants were harvested at 0, 1, 4, and 10 h after adding CHX. PRR5-GFP protein was analyzed by anti-GFP antibodies and quantitated relative to Coomassie-stained regions (*CBB*). Blots are representative of three trials. Means of three trials $\pm$ S.E. are shown. *E,* diurnal oscillation of PRR5 is diminished by *ztl-1*. Time course of PRR5-GFP protein levels in 10-day-old plants grown under LD cycles probed with anti-GFP antibodies. Coomassie-stained regions (*CBB*) are also shown. Blots are representative of more than three trials. Means of three trials $\pm$ S.E. are shown.

sistent with this notion, the free-running period in the *prr5 toc1* background is significantly shorter (18.4 h) than that of the *toc1* (19.9 h) and *prr5* (23.2 h) hours for the *toc1* single mutants (supplemental Fig. S2*B*) (50).

Blue Light Stabilizes PRR and ZTL Protein Levels—ZTL-mediated TOC1 degradation is thought to be facilitated by the dark, implying a potential protective role by light (33). We tested whether this is also true for PRR5, and whether proteolysis differs under different light qualities. Light-grown entrained plants were shifted to continuous dark, blue or red light and harvested at different times after CHX application at CT 19. In blue light, PRR5 was significantly more stable, relative to red light and darkness (Fig. 4*A*) (35). Interestingly, ZTL levels were also more stable under blue light, relative to red light, under the same conditions (Fig. 4*B*). These results support the notion that under blue light, degradation of PRR5 is inhibited,
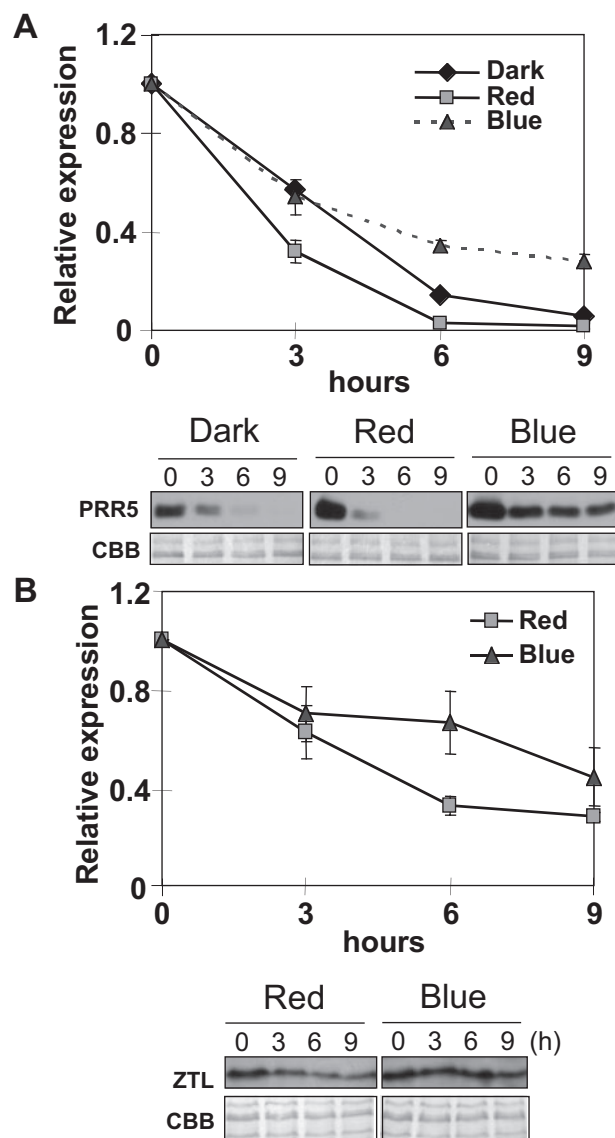
FIGURE 4. **PRR5 and ZTL are stabilized under blue light.** *A,* 10-day-old plants grown under LD cycles were transferred to continuous dark, red or blue light at ZT0 and treated with 100 μM CHX 19 h after transfer. Plants were harvested at 0, 3, 6, and 9 h after starting CHX treatment. PRR5-GFP protein was analyzed by anti-GFP antibodies and quantified relative to the Coomassie-stained region (*CBB*). *B,* ZTL protein is stabilized by blue light. Growth and tissue processing as in *A.* ZTL levels in extended darkness were too low to quantify. PRR5-GFP and ZTL protein immunoblots were quantified relative to Coomassie-stained regions (*CBB*) and normalized to time 0. Blots are representative of three trials. Means of three trials $\pm$ S.E. are shown.

possibly through a light-mediated disruption of the ZTL/PRR5 interaction.

Phosphorylation of the PRR proteins varies throughout the diurnal cycle. In other systems, phosphorylation of F-box protein targets is required to facilitate interaction (51, 52). To further dissect the nature of the ZTL/PRR5 interaction we first examined whether PRR5 is phosphorylated at any time during the circadian cycle. Immunoblots detecting PRR5-GFP showed at least two bands of distinctly different mobilities with a similar relative abundance of both present at all time points over a diurnal cycle (Fig. 5*A*). We next determined that both the upper and lower forms of PRR5-GFP are the result of greater and lesser degrees of protein phosphorylation, respectively.
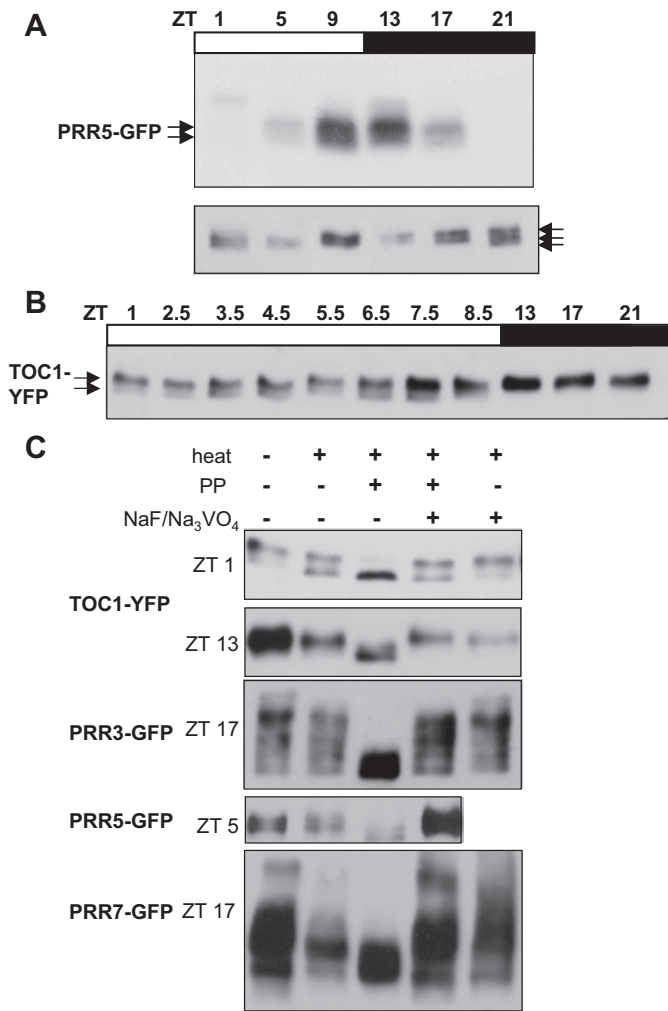
FIGURE 5. PRR proteins are phosphorylated. *A*, diurnal pattern of PRR5-GFP phosphorylation. *Upper panel*, equal loadings (60 μg) of protein from PRR5-GFP plants were probed with anti-GFP antibody at the time points indicated. *Lower panel*, loading amounts adjusted by dilution with WT extracts for better visualization of banding patterns at each time point. *B*, diurnal pattern of TOC1-yellow fluorescent protein (YFP) phosphorylation. Equal loadings (60 μg) of protein from TMG plants were probed with anti-GFP antibody at the time points indicated. ZT13 and -17 extracts were diluted 1:6 and ZT21 diluted 1:3 with WT extracts for better visualization. *C*, phosphorylation of PRR proteins. Extracts from the genotypes and time points indicated were treated with λ (TOC1, PRR5) or calf alkaline phosphatase (PRR3, PRR7) (*PP*) and/or phosphatase inhibitors (NaF/Na$_3$VO$_4$) and heat incubated prior to SDS-PAGE. *Arrowheads* indicate migration positions. Gel composition for TOC1-YFP, PRR5-GFP, and PRR3-GFP was 149:1 (acrylamide:bisacrylamide) and 37.5:1 for PRR7-GFP. All blots are representative of multiple trials.

Extracts treated with λ-PP shifted the PRR5-GFP mobility to lower than either of the two normally observable bands, indicating that both forms of PRR5-GFP are phosphorylated to some extent at nearly all times during the circadian cycle (Figs. 5*C* and 6*B*). Occasionally we observed a third, very rapidly migrating form at ZT21 that corresponds to the most dephosphorylated form of the protein (Fig. 5*A*).

Similar experiments were performed with TOC1-YFP extracts and we resolved two bands during the photoperiod (Fig. 5*B*). During the dark period, however, only a single, more slowly migrating band was detectable. Phosphatase treatment of TOC1-YFP extracts at ZT1 and ZT13 shows that the slower migration of the upper band results from phosphorylation (Fig.
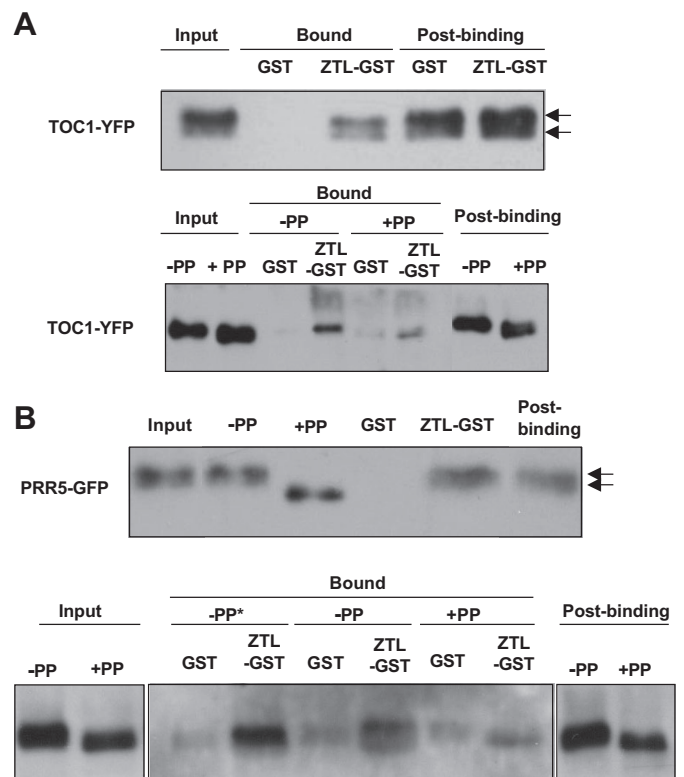
FIGURE 6. PRR5-GFP and TOC1-YFP *in vitro* binding to ZTL is enhanced by phosphorylation. *A*, binding of TOC1-yellow fluorescent protein (YFP) *Arabidopsis* protein extracts to ZTL-GST resin. TMG/*ztl-3* (*TOC1::TOC1-YFP* expressed in *ztl-3*) seedlings were entrained in LD cycles for 10 days and harvested at ZT13. Total protein was extracted with immunoprecipitation buffer and incubated with ZTL-GST resin (*upper panel*). ZTL-bound TOC1-YFP was detected with an anti-GFP antibody. Effects of phosphatase (*PP*) treatment on TOC1 binding to ZTL (*lower panel*). TMG seedlings were entrained in LD and harvested at ZT13. Total protein extracts were incubated with or without λ-protein phosphatase 15 min at 30 °C prior to incubation with ZTL-GST resin. *B*, binding of PRR5-GFP expressing *Arabidopsis* protein extracts to ZTL-GST resin. PRR5-GFP (*PRR5::PRR5-GFP*) expressed in wild type Columbia seedlings were entrained and harvested as in *A*. Total protein extract preparation, λ-PP treatment, incubation with ZTL-GST resin and sample separation (8% SDS-PAGE (acrylamide:bisacrylamide, 149:1)) are as described in *A*. PRR5-GFP was detected with an anti-GFP antibody. −*PP* and +*PP*, extracts incubated with or without λ-PP, respectively. −*PP**, extracts preincubated on ice prior to ZTL-GST resin incubation. *ZTL-GST*, ZTL-GST resin; *GST*, GST resin alone. All blots are representative of three trials.

5*C*). We also tested the PRR3-GFP and PRR7-GFP proteins for phosphorylation status. The multiple, ladder-like array of PRR3-GFP bands detectable during the dark period collapsed to essentially a single rapidly migrating band upon phosphatase treatment (Fig. 5*C*). Similarly, PRR7-GFP migration is increased in the presence of λ-phosphatase (Fig. 5*C*). Hence, all four PRR proteins undergo diurnal variation in both protein abundance and phosphorylation state.

Phosphorylation of TOC1 and PRR5 May Enhance ZTL Binding—We next tested whether the interaction of ZTL with the two PRR substrates (TOC1 and PRR5) is affected by phosphorylation status. Because both proteins show detectable differences in mobility we first tested binding to ZTL-GST using protein extracts from time points when both forms of the respective protein are detectable. Both the slower and faster migrating forms of TOC1-YFP can bind ZTL (Fig. 6*A*). When we then tested phosphatase-treated extracts compared with mock treated samples, both forms of TOC1-YFP bound to ZTL,

A

B
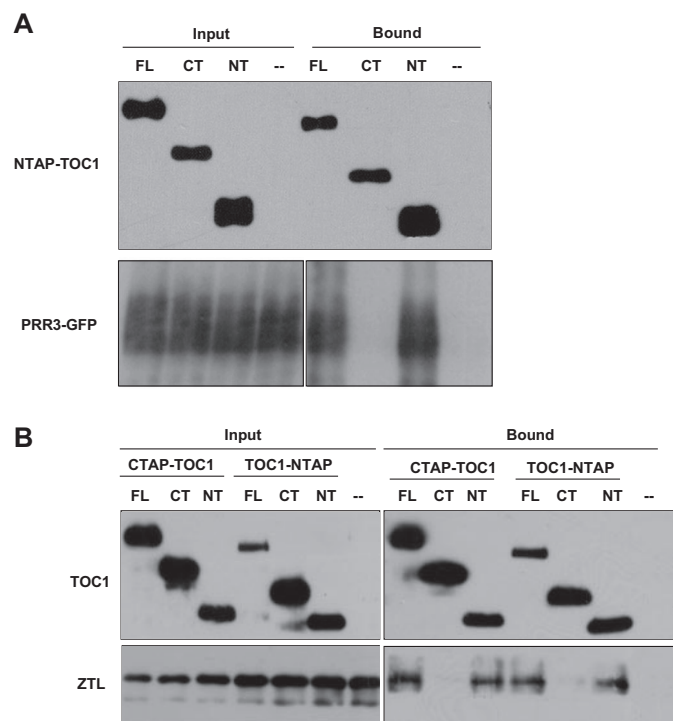
FIGURE 7. **The TOC1 N terminus is required for interaction with PRR3 and ZTL.** *A,* co-immunoprecipitation of full-length TAP-TOC1 (*FL*), TAP-TOC1 C terminus (*CT*), and TAP-TOC1 N terminus (*NT*) with PRR3-GFP. *Agrobacterium* expressing TAP-TOC1 and deletions were coinfiltrated with PRR3-GFP into *N. benthamiana* leaves. Total protein extracts were incubated with IgG-agarose and Precission protease-released immune complexes were separated by 6% SDS-PAGE. TAP tagged-TOC1 was detected with an anti-His antibody, whereas PRR3 was detected with an anti-GFP antibody. Both proteins were still present in post-binding supernatants (data not shown). *B,* co-immuno-precipitation of full-length (*FL*) TOC1 and TOC1 deletions with ZTL. Expression of TAP-TOC1 as in *A*. After 24 h, *Agrobacterium* expressing ZTL was infiltrated into the same leaves. Total protein extraction, IgG-agarose incubation, and protease-mediated release of immune complexes as in *A*. Input of TOC1 and its deletions was detected with an anti-PAP antibody, whereas immunoprecipitated TOC1 and its deletions were detected with an anti-His antibody. ZTL was detected with anti-ZTL antibody. −, co-infiltration of p19-expressing *Agrobacterium* with PRR3-GFP or ZTL used as a negative controls. All blots are representative of three trials.

although dephosphorylated TOC1-YFP appears to bind more weakly (Fig. 6*A*, *lower panel*).

Experiments with PRR5-GFP gave similar results. Both faster and slower migrating bands bound to ZTL-GST (Fig. 6*B*). PRR5-GFP from phosphatase-treated extracts still associated with ZTL-GST, but with reduced affinity. Together these results indicate that phosphorylated forms of both TOC1 and PRR5 bind ZTL, and that this modification may act to modulate their respective abundances.

Phosphorylation of TOC1 and PRR3 Is Necessary for Robust Interactions—PRR3 and TOC1 can interact in yeast and *in planta*, and PRR3 has been implicated in the stabilization of TOC1 protein (53). We examined whether the phosphorylation state of these proteins influences their interactions. First we established that TOC1 and PRR3 interact *in planta* through co-infiltration of TOC1 (TAP-TOC1) and PRR3 (PRR3-GFP) in *N. benthamiana* (Fig. 7). Full-length and the N terminus (amino acids 1–243) of TOC1 interact well with PRR3, whereas the TOC1 C terminus (amino acids 243– 648) shows no detectable affinity (Fig. 7*A*). Interestingly, this is the same region of TOC1 that interacts with ZTL (Fig. 7*B*).

We next bound TAP-TOC1 expressed in *N. benthamiana* to IgG resin and tested whether TOC1 phosphorylation affected *in vitro* binding of PRR3-GFP extracted from *Arabidopsis* seedlings. Pre-treatment of resin-bound TOC1 with λ-phosphatase resulted in a single, faster migrating TOC1 band upon protease-mediated release from the resin, indicating the effectiveness of the phosphatase treatment (Fig. 8*A*). Interaction between TOC1 and PRR3 is strongly diminished by this pre-treatment of TOC1 with phosphatase (Fig. 8*A*).

We next observed the relative binding affinity of PRR3-GFP from tissue harvested at different time points to phosphorylated TOC1-TAP. The strong diurnal and circadian-regulated progression of PRR3 phosphorylation over time (Fig. 1, *D* and *E*) suggested a way to assess relative binding affinity within a single extract. Although the less phosphorylated forms of PRR3 predominate at ZT10 and -13, there is a disproportionately larger fraction of more highly phosphorylated PRR3 bound to TOC1 at these times (Fig. 8*B*). Similarly, at ZT17, when highly phosphorylated PRR3 is most abundant, this form binds extremely well. In support of this finding, CIP pretreatment of PRR3-GFP *Arabidopsis* extracts results in the dephosphorylation of PRR3 and the subsequent loss of TOC1 binding (Fig. 8*C*). Taken together these results support the notion that phosphorylation of both TOC1 and PRR3 is necessary for optimal interaction.

PRR3 as an Inhibitor of the ZTL/TOC1 Interaction—TOC1 levels are diminished *in vivo* in the absence of PRR3, and levels are enhanced when PRR3 levels are enhanced. Additionally, yeast three-hybrid tests suggest that PRR3 might interfere with the TOC1/ZTL interaction (53). These reports, together with our above findings, recommended an *in planta* test of this hypothesis. We co-expressed GFP-PRR3, TAP-TOC1, and ZTL in *N. benthamiana* and observed the amount of ZTL co-immunoprecipitated with TOC1 in the presence and absence of PRR3. PRR3 diminished the relative amount of ZTL found in association with TOC1. Similar tests using only the N terminus of TOC1 gave similar results (Fig. 9). Because the same N-terminal region of TOC1 interacts with ZTL and PRR3, these results are consistent with PRR3 acting to competitively inhibit the ZTL/TOC1 interaction, contributing to the phase-specific enhancement of TOC1 levels.

DISCUSSION

To determine additional targets of the F-box protein ZTL and understand their post-translational regulation, we have characterized the five PRR proteins in *Arabidopsis* that previously have been identified as components of the plant circadian clock (10–12, 44, 46, 54, 55). The high amplitude cycling of the PRR proteins, which lag behind the respective message levels, demonstrates a rapid turnover of all five proteins, indicating a highly regulated control of protein abundance. High level ectopic expression of these proteins have marked effects on the circadian period but these previous studies altered both the phase and level of expression (43, 49, 56, 57). Results presented here, together with the *prr* mutant phenotypes, suggest a strong significance to the high amplitude, phase-specific expression of the PRR proteins.
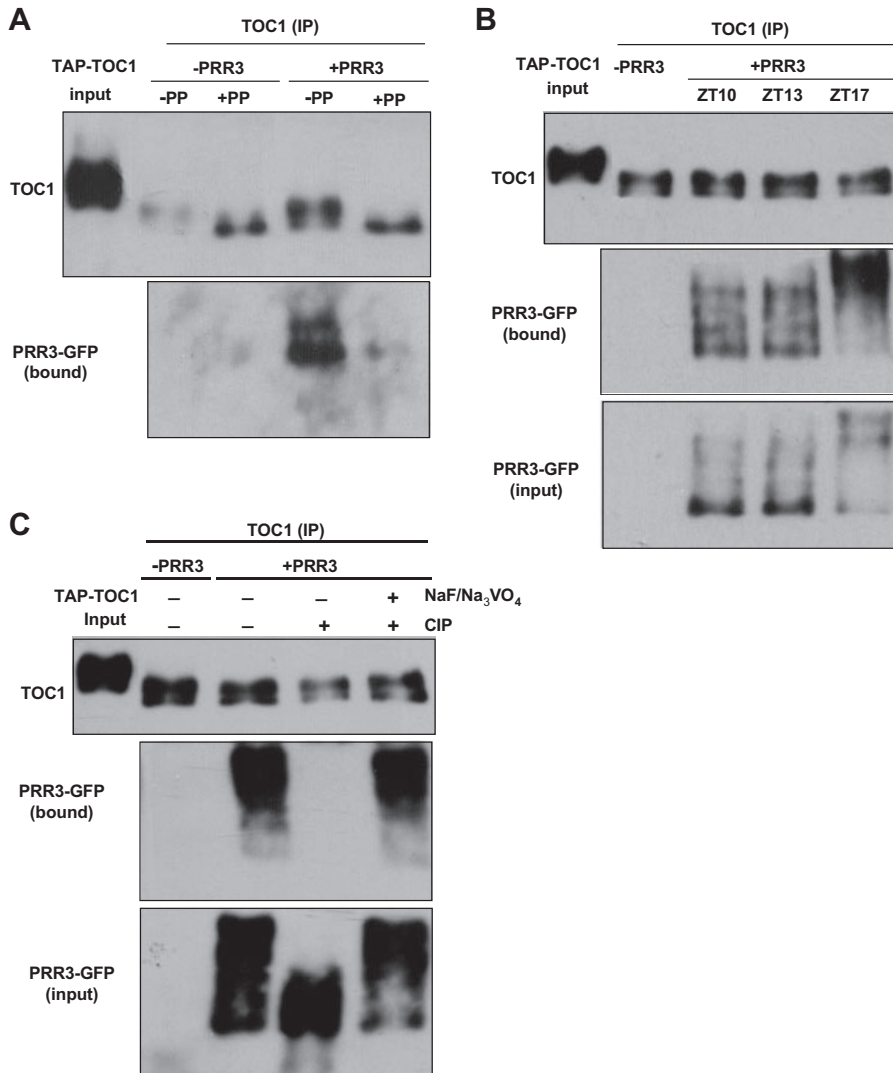
FIGURE 8. **Phosphorylation is essential for TOC1 and PRR3 interaction *in vitro*.** *A*, TAP-TOC1 *in vitro* binding of PRR3 is decreased by TOC1 dephosphorylation. Pre-loading of IgG-agarose with TAP-TOC1 was performed by incubation of the agarose with *N. benthamiana* total protein extracts transiently expressing full-length TAP-TOC1. Protein extracts from *PRR3::PRR3-GFP* expressing *Arabidopsis* seedlings were incubated with TAP-TOC1-bound agarose resin pre-treated with λ-phosphatase (λ-*PP*) or mock treated. Immune complexes were released with Precission protease, separated by SDS-PAGE. −*PP* and +*PP*, resin incubated without or with λ-PP, respectively. −*PRR3*, wild type *Arabidopsis* extracts. Precission protease treatment release of TOC1 from the resin results in a faster migrating form of TOC1 in the immunoprecipitation (*IP*) lanes. TOC1 was detected with an anti-His antibody and PRR3 was detected with an anti-GFP antibody. *B*, TAP-TOC1 predominantly binds phosphorylated PRR3. *PRR3::PRR3-GFP* seedlings were entrained in LD for 6 days and harvested at the indicated time points. Pre-loading of IgG-agarose with TAP-TOC1, incubation with PRR3-GFP extracts from *Arabidopsis*, release of immune complexes, and sample separation by SDS-PAGE were performed as in *A*. TOC1 and PRR3 were detected as in *A*. −*PRR3*, wild type plants harvested at ZT13. *C*, TOC1 *in vitro* binding of PRR3 requires PRR3 phosphorylation. *PRR3::PRR3-GFP* seedlings grown as in *B* and harvested at ZT17. Pre-loading of IgG-agarose with TAP-TOC1, incubation with PRR3-GFP extracts from *Arabidopsis*, release of immune complexes, and sample separation by SDS-PAGE performed as in *A*. PRR3-GFP protein extracts were incubated with or without CIP at 37 °C for 15 min. *NaF* and *Na₃VO₄*, phosphatase inhibitors. −*PRR3*, wild type plants. TOC1 and PRR3 were detected as in *A*. Representative of three trials is shown. In all cases PRR3-GFP was still present in post-binding supernatants (data not shown).

ZTL Targets a Subset of Late-phased PRR Proteins to Control Circadian Period—Through combined approaches involving examination of gene expression patterns, *in vivo* protein-protein interactions, and genetics we have delimited the PRR target substrates of ZTL to TOC1 and PRR5, confirming and extending previous reports (33, 35). Both proteins have very similar phases of expression and act similarly to lengthen the free-running period. The additivity of their mutant circadian pheno-

types suggests they may be part of a common complex, which may have diminished activity in the absence of one or the other, or they may participate in separate, similarly acting complexes. Further identification of TOC1 and PRR5 interactors will be necessary to resolve these possibilities. Previous studies have demonstrated the severe loss of circadian cycling in *prr5 prr7* and *prr5 prr7 prr9* mutants (13, 14). These results are consistent with multiloop models where early phased and late phased PRR proteins comprise two separate functional groups, implying that the simultaneous loss of single members from both groups should have a more severe reduction of circadian function than double mutants within either of the two groups (5, 6, 54). The different combinations of late phased *toc1*, *prr3*, and *prr5* mutants examined here do not result in rapid damping but are simply a shorter period. These data are consistent with the notion that these three proteins together comprise, or are part of, a functional unit of the circadian oscillator.

Light-dependent Regulation of ZTL Targets—TOC1 and *PRR5* mRNA and protein show maximal expression during the subjective night, in phase with ZTL peak expression (31). This is unexpected given that high levels of ZTL should result in concomitantly low substrate (TOC1 and PRR5) levels. The greater stability of PRR5 in blue light is consistent with the increased PRR5/ZTL interaction we observed in the dark (Fig. 3*C*), with both results implying an inhibition of interaction and degradation of PRR5 in the light. The greater stability of ZTL under blue light further suggests the presence of a factor that simultaneously stabilizes ZTL but restricts targeting of PRR5 for degradation. A strong candidate for this factor is GI. Recently, we have identified GI as a post-translational stabilizer of ZTL through an interaction enhanced by blue-light dependent activation of the ZTL LOV domain (42). GI binding via the LOV motif may thus simultaneously stabilize ZTL while conformationally blocking access of ZTL substrates to the kelch interaction region. The GI/ZTL interaction would allow the increase of all four proteins (GI, ZTL, TOC1, and PRR5) during the

PRR Protein Phosphorylation
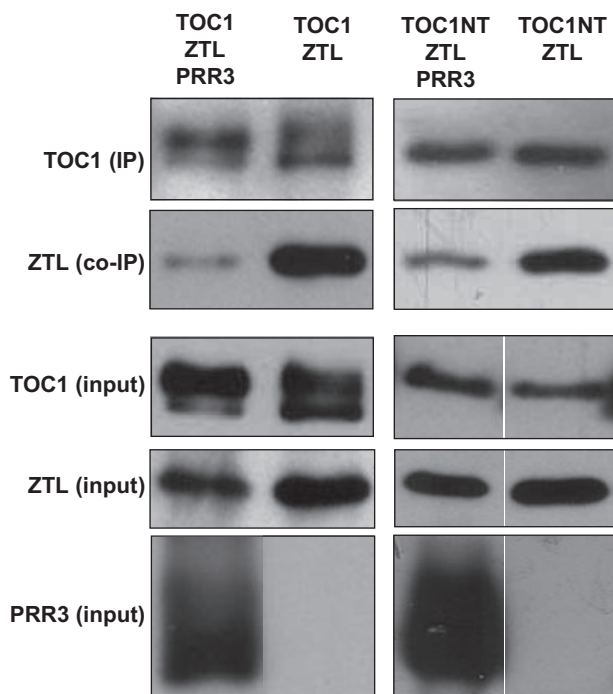
FIGURE 9. **TOC1/ZTL interaction is diminished by PRR3.** ZTL and TAP fusions of full-length or N terminus TOC1 were co-expressed with or without GFP-PRR3 in *N. benthamiana* using the same techniques and constructs as previously described, and protein extracts were used for immunoprecipitation (*IP*) by IgG-agarose. TAP immune complexes probed for TAP-TOC1 and co-immunoprecipitated (*co-IP*) ZTL are shown. *TOC1*, TAP-TOC1; *TOC1NT*, TAP-TOC1 N terminus; *PRR3*, GFP-PRR3. Representative of three trials is shown. All proteins were still present in post-binding supernatants (data not shown).

FIGURE 10. **Post-translational fine tuning of clock protein oscillations by phosphorylation-dependent competitive interactions.** ZTL targets TOC1 to proteasome-dependent degradation through direct interaction. TOC1 and PRR3 proteins are phosphorylated and their phosphorylation state varies diurnally and circadianly. Early after lights-on, TOC1 is expressed at low levels in both a lesser (or non-) and the greater phosphorylated form, whereas the latter form is only present during the night. Similarly, PRR3 protein shows ladder-like multiply phosphorylated forms predominately at night. TOC1, PRR3, and ZTL all show diurnal protein levels peaking around ZT13. Although the ZTL/TOC1 interaction is slightly enhanced by TOC1 phosphorylation, the phosphorylated forms of TOC1 and PRR3 strongly preferentially interact. In this model, ZTL and PRR3 compete for interaction with the N terminus of TOC1, and following the enhancement of the TOC1/PRR3 interaction through phosphorylation, this pairing results in greater TOC1 stabilization by competitively blocking the ZTL/TOC1 interaction. The *black bar* indicates night.

photoperiod, followed by the dissociation of GI and ZTL in the dark, freeing ZTL to associate with and degrade the PRR substrates. Thus a combination of clock-controlled phasing of transcription (GI, TOC1, and PRR5) together with blue light-enhanced interaction and stabilization (GI and ZTL) could result in the similarly late phased, high amplitude cycling observed for these essential clock components.

Indirect Transcriptional Regulation of PRR9 by ZTL—Two previous reports have described the strong suppression of *PRR9* message levels when TOC1 and PRR5 are strongly overexpressed (49, 56). Our results, and others, support these ectopic studies by showing that when TOC1 and PRR5 levels rise and lose their distinctly phased expression patterns in *ztl* mutants PRR9 expression is strongly dampened. These data demonstrate how ZTL, through its role in the control of PRR5 and TOC1 protein levels, indirectly controls the phase and amplitude of *PRR9* expression. Current computational models of the plant circadian clock are comprised of three or four interlocked loops, incorporating five known components (LHY/CCA1, PRR7/PRR9, and TOC1) along with a number of hypothetical factors, and these models are largely built around transcriptional activation and repression (5, 6). Our results make explicit the central role of protein stability in the control of transcription and in circadian timing.

Roles for Phosphorylation of TOC1 and PRR5—During the photoperiod, TOC1 exists in two states of either lesser or greater phosphorylation, but appears in the more fully phosphorylated form during the dark period. In contrast, PRR5 displays two phosphorylation states nearly unchanged in relative abundance during the entire diurnal cycle. One possible function of the phosphorylation is enhanced binding to ZTL, because in yeast and other systems substrate phosphorylation generally enhances interaction with the cognate F-box proteins (51). However, recent reports from plant systems indicate this is not always the case. The *Arabidopsis* AUX/IAA proteins do not appear to require phosphorylation for binding and subsequent ubiquitylation by the TIR1 family of F-box proteins (58). Similarly, the DELLA substrate of the rice SCF^{GID2} complex, SLR1, binds to GID2 in both the phosphorylated and unphosphorylated forms (59, 60). Our findings support these results, as TOC1 and PRR5 interactions with ZTL are only mildly affected by their phosphorylation status, with slightly higher binding correlating with a more phosphorylated forms.

More significant is the strong effect of phosphorylation on the promotion of the PRR3 and TOC1 interaction. This finding correlates very well with the coincidence *in vivo* of an advanced level of PRR3 phosphorylation with the more highly phosphorylated form of TOC1 late in the subjective night. The notion that an enhanced interaction between PRR3 and TOC1 during this time results in protection of TOC1 from degradation by ZTL is consistent with a recent report demonstrating higher levels of TOC1 in a PRR3 overexpressor and reduced TOC1 in the *prr3* mutant (53) (see Fig. 10). Furthermore, the N terminus of TOC1 is required for both the PRR3 and ZTL interaction, establishing this domain as critical to sustaining the appropriate TOC1 levels necessary for proper circadian function. Fur-

ther studies will define the kinases responsible for PRR3 and TOC1 regulation and how subcellular levels of TOC1 may be controlled by phosphorylation-dependent interactions.

REFERENCES

1. Johnson, C. H., and Kyriacou, C. (2005) in *Endogenous Plant Rhythms* (Hall, A., and McWatters, H., eds) pp. 237–260, Blackwell, Oxford
2. Dodd, A. N., Salathia, N., Hall, A., Kevei, E., Toth, R., Nagy, F., Hibberd, J. M., Millar, A. J., and Webb, A. A. (2005) *Science* **309,** 630–633
3. Green, R. M., Tingay, S., Wang, Z. Y., and Tobin, E. M. (2002) *Plant Physiol.* **129,** 576–584
4. Alabadi, D., Oyama, T., Yanovsky, M. J., Harmon, F. G., Mas, P., and Kay, S. A. (2001) *Science* **293,** 880–883
5. Locke, J. C., Kozma-Bognar, L., Gould, P. D., Feher, B., Kevei, E., Nagy, F., Turner, M. S., Hall, A., and Millar, A. J. (2006) *Mol. Syst. Biol.* **2,** 59
6. Zeilinger, M. N., Farre, E. M., Taylor, S. R., Kay, S. A., and Doyle, F. J., III (2006) *Mol. Syst. Biol.* **2,** 58
7. Matsushika, A., Makino, S., Kojima, M., and Mizuno, T. (2000) *Plant Cell Physiol.* **41,** 1002–1012
8. Yamamoto, Y., Sato, E., Shimizu, T., Nakamich, N., Sato, S., Kato, T., Tabata, S., Nagatani, A., Yamashino, T., and Mizuno, T. (2003) *Plant Cell Physiol.* **44,** 1119–1130
9. Kaczorowski, K. A., and Quail, P. H. (2003) *Plant Cell* **15,** 2654–2665
10. Michael, T. P., Salome, P. A., Yu, H. J., Spencer, T. R., Sharp, E. L., McPeek, M. A., Alonso, J. M., Ecker, J. R., and McClung, C. R. (2003) *Science* **302,** 1049–1053
11. Salome, P. A., and McClung, C. R. (2005) *Plant Cell* **17,** 791–803
12. Farre, E. M., Harmer, S. L., Harmon, F. G., Yanovsky, M. J., and Kay, S. A. (2005) *Curr. Biol.* **15,** 47–54
13. Nakamichi, N., Kita, M., Ito, S., Sato, E., Yamashino, T., and Mizuno, T. (2005) *Plant Cell Physiol.* **46,** 609–619
14. Nakamichi, N., Kita, M., Ito, S., Yamashino, T., and Mizuno, T. (2005) *Plant Cell Physiol.* **46,** 686–698
15. Ito, S., Matsushika, A., Yamada, H., Sato, S., Kato, T., Tabata, S., Yamashino, T., and Mizuno, T. (2003) *Plant Cell Physiol.* **44,** 1237–1245
16. Eriksson, M. E., Hanano, S., Southern, M. M., Hall, A., and Millar, A. J. (2003) *Planta* **218,** 159–162
17. Harmer, S. L., Panda, S., and Kay, S. A. (2001) *Annu. Rev. Cell Dev. Biol.* **17,** 215–253
18. Bell-Pedersen, D., Cassone, V. M., Earnest, D. J., Golden, S. S., Hardin, P. E., Thomas, T. L., and Zoran, M. J. (2005) *Nat. Rev. Genet.* **6,** 544–556
19. Brunner, M., and Schafmeier, T. (2006) *Genes Dev.* **20,** 1061–1074
20. Liu, Y. (2005) *Methods Enzymol.* **393,** 379–393
21. Fang, Y., Sathyanarayanan, S., and Sehgal, A. (2007) *Genes Dev.* **21,** 1506–1518
22. Godinho, S. I., Maywood, E. S., Shaw, L., Tucci, V., Barnard, A. R., Busino, L., Pagano, M., Kendall, R., Quwailid, M. M., Romero, M. R., O'neill, J., Chesham, J. E., Brooker, D., Lalanne, Z., Hastings, M. H., and Nolan, P. M. (2007) *Science* **316,** 897–900
23. Siepka, S. M., Yoo, S. H., Park, J., Song, W., Kumar, V., Hu, Y., Lee, C., and Takahashi, J. S. (2007) *Cell* **129,** 1011–1023
24. Ko, H. W., Jiang, J., and Edery, I. (2002) *Nature* **420,** 673–678
25. Daniel, X., Sugano, S., and Tobin, E. M. (2004) *Proc. Natl. Acad. Sci. U. S. A.* **101,** 3292–3297
26. Sugano, S., Andronis, C., Ong, M. S., Green, R. M., and Tobin, E. M. (1999) *Proc. Natl. Acad. Sci. U. S. A.* **96,** 12362–12366
27. Sugano, S., Andronis, C., Green, R. M., Wang, Z. Y., and Tobin, E. M. (1998) *Proc. Natl. Acad. Sci. U. S. A.* **95,** 11020–11025
28. David, K. M., Armbruster, U., Tama, N., and Putterill, J. (2006) *FEBS Lett.* **580,** 1193–1197
29. Perales, M., Portoles, S., and Mas, P. (2006) *Plant J.* **46,** 849–860
30. Song, H. R., and Carre, I. A. (2005) *Plant Mol. Biol.* **57,** 761–771
31. Kim, W. Y., Geng, R., and Somers, D. E. (2003) *Proc. Natl. Acad. Sci. U. S. A.* **100,** 4933–4938
32. Han, L., Mason, M., Risseeuw, E. P., Crosby, W. L., and Somers, D. E. (2004) *Plant J.* **40,** 291–301
33. Mas, P., Kim, W. Y., Somers, D. E., and Kay, S. A. (2003) *Nature* **426,** 567–570
34. Somers, D. E., Schultz, T. F., Milnamow, M., and Kay, S. A. (2000) *Cell* **101,** 319–329
35. Kiba, T., Henriques, R., Sakakibara, H., and Chua, N. H. (2007) *Plant Cell* **19,** 2516–2530
36. Curtis, M. D., and Grossniklaus, U. (2003) *Plant Physiol.* **133,** 462–469
37. Bechtold, N., Ellis, J., and Pelletier, G. (1993) *C. R. Acad. Sci. (Paris)* **316,** 1194
38. Ding, Z., Doyle, M. R., Amasino, R. M., and Davis, S. J. (2007) *Genetics* **176,** 1501–1510
39. Somers, D. E., Kim, W. Y., and Geng, R. (2004) *Plant Cell* **16,** 769–782
40. Guo, F. Q., Wang, R., Chen, M., and Crawford, N. M. (2001) *Plant Cell* **13,** 1761–1777
41. Zachgo, S., Perbal, M. C., Saedler, H., and Schwarz-Sommer, Z. (2000) *Plant J.* **23,** 697–702
42. Kim, W. Y., Fujiwara, S., Suh, S. S., Kim, J., Kim, Y., Han, L., David, K., Putterill, J., Nam, H. G., and Somers, D. E. (2007) *Nature* **449,** 356–360
43. Matsushika, A., Murakami, M., Ito, S., Nakamichi, N., Yamashino, T., and Mizuno, T. (2007) *Biosci. Biotechnol. Biochem.* **71,** 527–534
44. Farre, E. M., and Kay, S. A. (2007) *Plant J.* **52,** 548–560
45. Ito, S., Nakamichi, N., Kiba, T., Yamashino, T., and Mizuno, T. (2007) *Plant Cell Physiol.* **48,** 1644–1651
46. Strayer, C., Oyama, T., Schultz, T. F., Raman, R., Somers, D. E., Mas, P., Panda, S., Kreps, J. A., and Kay, S. A. (2000) *Science* **289,** 768–771
47. Matsushika, A., Kawamura, M., Nakamura, Y., Kato, T., Murakami, M., Yamashino, T., and Mizuno, T. (2007) *Biosci. Biotechnol. Biochem.* **71,** 535–544
48. Kevei, E., Gyula, P., Hall, A., Kozma-Bognar, L., Kim, W. Y., Eriksson, M. E., Toth, R., Hanano, S., Feher, B., Southern, M. M., Bastow, R. M., Viczian, A., Hibberd, V., Davis, S. J., Somers, D. E., Nagy, F., and Millar, A. J. (2006) *Plant Physiol.* **140,** 933–945
49. Makino, S., Matsushika, A., Kojima, M., Yamashino, T., and Mizuno, T. (2002) *Plant Cell Physiol.* **43,** 58–69
50. Ito, S., Niwa, Y., Nakamichi, N., Kawamura, H., Yamashino, T., and Mizuno, T. (2008) *Plant Cell Physiol.* **49,** 201–213
51. Willems, A. R., Schwab, M., and Tyers, M. (2004) *Biochim. Biophys. Acta* **1695,** 133–170
52. Smalle, J., and Vierstra, R. D. (2004) *Annu. Rev. Plant Biol.* **55,** 555–590
53. Para, A., Farre, E. M., Imaizumi, T., Pruneda-Paz, J. L., Harmon, F. G., and Kay, S. A. (2007) *Plant Cell* **19,** 3462–3473
54. Mizuno, T., and Nakamichi, N. (2005) *Plant Cell Physiol.* **46,** 677–685
55. McClung, C. R. (2006) *Plant Cell* **18,** 792–803
56. Sato, E., Nakamichi, N., Yamashino, T., and Mizuno, T. (2002) *Plant Cell Physiol.* **43,** 1374–1385
57. Matsushika, A., Imamura, A., Yamashino, T., and Mizuno, T. (2002) *Plant Cell Physiol.* **43,** 833–843
58. Dharmasiri, N., Dharmasiri, S., Jones, A. M., and Estelle, M. (2003) *Curr. Biol.* **13,** 1418–1422
59. Ueguchi-Tanaka, M., Nakajima, M., Motoyuki, A., and Matsuoka, M. (2007) *Annu. Rev. Plant Biol.* **58,** 183–198
60. Itoh, H., Sasaki, A., Ueguchi-Tanaka, M., Ishiyama, K., Kobayashi, M., Hasegawa, Y., Minami, E., Ashikari, M., and Matsuoka, M. (2005) *Plant Cell Physiol.* **46,** 1392–1399